ISSN 2070-0482, Mathematical Models and Computer Simulations, 2024, Vol. 16, No. 2, pp. 223–234. © Pleiades Publishing, Ltd., 2024.
Russian Text © The Author(s), 2023, published in Matematicheskoe Modelirovanie, 2023, Vol. 35, No. 11, pp. 103–121.

Modification of the Wilson–Frankel Kinetic Model and Atomistic Simulation of the Rate of Melting/Crystallization of Metals

V. I. Mazhukin[a], A. V. Shapranov[a], O. N. Koroleva[a,*], and A. V. Mazhukin[a]

[a] *Keldysh Institute of Applied Mathematics, Russian Academy of Sciences, Moscow, Russia*

**e-mail: koroleva.on@mail.ru*

Received December 5, 2022; revised June 19, 2023; accepted July 3, 2023

Abstract—Within the kinetic-atomistic approach, a new approach is proposed for constructing the temperature dependence of the stationary velocity of propagation of the solid–liquid interface (SLI) in metals: aluminum, copper, and iron with different crystallographic orientations. The considered temperature range includes the range of maximum allowable overheating/overcooling values for each of the metals. A significant modification to the well-known kinetic model with the Wilson–Frenkel (WF) diffusion constraint, which is used to construct the response function, is made. An atomistic simulation of the processes of melting/crystallization of metals aluminum, copper, and iron is carried out over the entire temperature range using three interaction potentials of the "embedded atom" family. By comparing the simulation results with the data of the modified kinetic model, the response function of the interface velocity in the range of maximum allowable overheating/overcooling values in metals is constructed using the least squares criterion. The use of the modified WF kinetic model in calculations significantly improves the accuracy of the response function over the considered temperature range. The resulting temperature dependence of the interface velocity is diffusion-limited and is described by the same equation for each metal over the considered temperature range.

Keywords: kinetic model, atomistic modeling, solid–liquid interface, velocity of the interface, overheating/overcooling

DOI: 10.1134/S207004822402011X

1. INTRODUCTION

The mechanisms of the melting of a solid body and solidification of a liquid are actively studied [1] phenomena. In recent years, extensive experimental [2–4] and theoretical studies coupled with modeling the melting/crystallization of solids [5–12] have significantly expanded the understanding of the nature of this phenomenon. There are two known mechanisms of melting/crystallization of solids–liquids: heterogeneous (surface or frontal) and homogeneous (volumetric). In the first case, the melting of solids and solidification of liquids are related to phase transformations of the first kind, in which, in contrast to the homogeneous mechanism, the phenomena of heterogeneous melting and solidification are always spatially heterogeneous. They correspond to the movement of a continuous medium with a strong discontinuity surface, on which the mechanical, thermodynamic, thermophysical, and optical characteristics of the substance change abruptly. Homogeneous melting/crystallization mechanisms, characterized by the nucleation of a new phase (liquid/crystal) in a certain volume of an overheated crystal or supercooled melt, deserve separate consideration. This article will discuss the mechanisms of heterogeneous melting.

Within classical thermodynamics [13], in heterogeneous melting/crystallization, phase equilibrium is achieved at a certain (equilibrium) temperature T_m, which at the phase front corresponds to the equality of the Gibbs free energies of the solid and liquid states.

The front temperature's deviation $T_{s\ell}$ from the equilibrium value T_m upward $T_{s\ell} > T_m$ or reduction $T_{s\ell} < T_m$ causes overheating/overcooling of the front and leads to movement of the interphase boundary (solid–liquid interface (SLI)). The SLI velocity of motion is a response function $v(T_{s\ell})$ of interface to overheating of the solid or undercooling of the liquid phase. The values of the maximum overheating and undercooling of the initial phase are related to the velocity of motion of the phase front $v(T_{s\ell})$. The overcooled and overheated states in the initial phase in the region of the melting/crystallization phase transition are manifested in the phenomenon of thermal hysteresis, which makes it possible to obtain estimates

of the values of the limiting overheating and undercooling of the initial phase [7, 8, 14, 15]. The velocity of motion of the interphase boundary $v(T_{s\ell})$ is a fundamental quantity describing the processes of crystallization and melting, and plays a fundamental role in materials science [5, 6].

A significant part of the dynamics of melting and crystal growth from the melt is determined by the heat transfer from the moving interface. However, there are limiting circumstances in which the growth rate is regulated not only by the macroscopic heat flow. One of these circumstances is the occurrence of fast phase transitions of the first kind, characteristic of the pulsed action of concentrated energy flows on materials, whose processes have their own specifics [4, 5]. Fast phase transitions are accompanied by the appearance of metastable highly overheated/supercooled states [7, 8, 14, 15], leading to a number of interface instabilities.

At the same time, the widespread use of lasers with ultrashort (picofemtosecond radiation range) pulses for processing various materials [12, 16] stimulates increased interest in fast first-order phase transitions. Analysis of the processes caused by pulsed laser exposure leads to the consideration of a number of important fundamental problems, which at high heating rates include the features of homogeneous and heterogeneous mechanisms of melting/solidification and evaporation, as well as the related extreme overheating and overcooling of the substance. Understanding melting/solidification processes is also of great interest for applied problems in photonics [17], ultrafast laser microprocessing of materials [16, 18], generation of nanoparticles and nanostructures [19, 20], etc.

In theoretical studies of the mobility of the solid–liquid interface and the related kinetics of crystal and melt growth, kinetic models [21–23] and atomistic modeling [24–26] are widely used. In most kinetic models, studies of the temperature dependence of stationary velocity $v(T_{s\ell})$ are still carried out predominantly in the crystallization temperature range. Therefore, for a number of materials, the determination of the temperature dependence of the velocity of motion of an SLI $v(T_{s\ell})$ throughout the entire superheat range remains an urgent problem: from the minimum value near the melting point T_m to the maximum near the spinodal.

The main tool for studying the kinetic rate of melting/crystallization in the region of maximum permissible values of overheating/overcooling is atomistic modeling, and its results are compared with the data of kinetic models. Achieving an acceptable fit is achieved by introducing appropriate correction parameters in the model [24–27].

The main aim of this study is to construct a modified kinetic model with diffusion limitation [28–30] with its subsequent application to metals: aluminum (Al), copper (Cu), and iron (Fe).

The developed model is focused on describing the mobility of an SLI in various metal crystals (Al, Cu (face-centered cubic (FCC) lattice), and Fe (body-centered cubic (BCC) lattice)) in a wide temperature range, including areas of the maximum permissible values of overheating/undercooling. A detailed study of the mobility of the kinetic properties of SLI metals using atomistic modeling with the subsequent comparison of the results obtained with the data of the developed kinetic model will make it possible to construct analytical temperature dependencies of the stationary velocity $v(T_{s\ell})$ in the area of the maximum permissible values of overheating/undercooling.

2. KINETIC DESCRIPTION OF SLI MOBILITY

Kinetic theories depicting temperature dependences of SLI mobility $v_{s\ell} = v(T_{s\ell})$ are based on various physical phenomena. The most well-known among them are the classical Wilson–Frenkel (WF) theory [28–30] with a diffusion mechanism for controlling the kinetics of the interphase boundary, a kinetic model with a collisional-thermal mechanism (Broughton, Gilmer, and Jackson (BGJ) [31, 32]), and the kinetic density functional theory (DFT) [23, 33], taking into account the influence of density changes.

The kinetic theory of WF [28–30] is based on the hypothesis that melting or solidification occurs through some intermediate or transition state; therefore, it is often called the transition state theory. In this theory, the SLI rate is controlled by a diffusion limitation mechanism based on the assumption that atoms (molecules) of the diffusion barrier during the transition from the liquid to the solid phase. The transition is accompanied by a significant restructuring of the interface. The rate of the crystallization process is assumed to be proportional to the diffusion coefficient, which is usually presented in the form of the Arrhenius equation

$$D = D_0 \exp\left(-Q^{\mathrm{WF}}/(k_B T_{s\ell})\right), \tag{1}$$

where Q^{WF} is the activation energy for motion of diffusion in a liquid, k_{B} is the Boltzmann constant, $k_{\mathrm{B}}T$ is the average thermal energy for one atom, and D_0 is a preexponent, having the dimension of a diffusion coefficient [m^2/s].

The temperature dependence of the velocity of the crystallization/melting front $v(T_{s\ell})$ in a model with diffusion limitation in a generalized form taking into account (1) is expressed by the equation

$$\begin{aligned} v(T_{s\ell}) &= \frac{af_0}{\lambda^2} D\left[1-\exp\left(-\frac{\Delta G}{k_B T_{s\ell}}\right)\right] \\ &= \frac{a^2 f_0}{\lambda^2}\frac{D_0}{a}\exp\left(-\frac{Q^{\mathrm{WF}}}{k_B T_{s\ell}}\right)\left[1-\exp\left(-\frac{L_m}{k_B T_m}\frac{\Delta T}{T_{s\ell}}\right)\right] \\ &= C^{\mathrm{WF}}_{\langle hk\ell\rangle}\exp\left(-\frac{Q^{WF}}{k_B T_{s\ell}}\right)\left[1-\exp\left(-\frac{L_m}{k_B T_m}\frac{\Delta T}{T_{s\ell}}\right)\right], \end{aligned} \tag{2}$$

where $C^{\mathrm{WF}}_{\langle hk\ell\rangle} = [(a^2/\lambda^2)f_0]D_0/a$ [m/sec], a is the interatomic distance, λ is the mean free path of atoms for this process and it is assumed that it is proportional to the lattice parameter, a: $\lambda < a$, f_0 is the efficiency coefficient (constant of the order of unity $f_0 < 1$) characterizing the proportion of collisions of liquid atoms with a solid substance leading to crystallization, and $\langle hk\ell\rangle$ are indices characterizing the anisotropy of the coefficient $C^{\mathrm{WF}}_{\langle hk\ell\rangle}$. The value of $C^{\mathrm{WF}}_{\langle hk\ell\rangle}$, depending on the crystallographic orientation of the interface [34], and the activation energy Q^{WF} are unknown and to be determined.

The BGJ theory [31] uses the frequency of thermal collisions of atoms with the interface as the SLI rate limit [35]. This theory was presented by the authors as a modification of the earlier WF theory. The results of molecular dynamics (MD) of the simulation [31] performed with a nonmetallic Lennard–Jones potential, which showed that crystal growth of monatomic systems may not in all cases be limited by diffusion, served as motivation. In particular, in the region of very low temperatures, the diffusion coefficient tends to zero, but according to the simulation results, the SLI rate still remains finite and the WF model turns out to be invalid. Following the hypothesis [35] that the solidification of monatomic metals is limited only by the frequency of collisions of the melt's atoms with the crystal surface, the authors of the BGJ model [31] replaced the diffusion term in (2) with the average thermal velocity of atoms $v_T = \sqrt{3k_B T_{s\ell}/m}$,

$$\begin{aligned} v\left(T_{s\ell}\right) &= \frac{a}{\lambda} f_0 v_T\left[1-\exp\left(-\frac{L_m}{k_B T_m}\frac{\Delta T}{T_{s\ell}}\right)\right] \\ &= C^{\mathrm{BGJ}}_{\langle hk\ell\rangle}\sqrt{\frac{3k_B T_{s\ell}}{m}}\left[1-\exp\left(-\frac{L_m}{k_B T_m}\frac{\Delta T}{T_{s\ell}}\right)\right], \end{aligned} \tag{3}$$

where $C^{\mathrm{BGJ}}_{(hk\ell)} = (a/\lambda)f_0$ is a dimensionless coefficient and m is the atomic mass.

The possibility of using the considered kinetic models WF, BGJ, DFT in the range of values close to the melting temperature to describe the crystallization process was considered in later works [26, 35, 37], in which atomistic modeling resulted in acceptable accuracy.

With the development of more accurate multiparticle potentials for metals, a number of MD studies of crystal growth in pure metals have been carried out at various supercooling temperature ranges. Atomistic modeling [36, 38] showed that in the range of values close to the melting temperature, the crystallization process can be represented with acceptable accuracy by kinetic models with diffusion (2) and collisional-thermal limitations (3), as well as DFT models [23, 33]. For deep supercoolings, it is preferable [36, 38] to use a kinetic model with collisional-thermal limitation [31] and an Arrhenius-type model [38]. In the region of intermediate supercooling at a level of ~$0.7T_m$, the advantage remains with the WF diffusion-limited transition state model. In [39], a specially developed semiempirical potential was used to simulate the phase transformation in a disordered one-component system. The simulation showed that the WF theory satisfactorily describes the results of the MD simulation of interface migration in the temperature range from $0.55T_m$ to T_m, while the BGJ theory is less accurate in describing the temperature dependence of the SLI rate in the same temperature range. Below $0.55T_m$, none of the existing theories are capable of reproducing the temperature dependence of the interface velocity.

A significantly smaller number of works [27, 40, 49, 50] analyze the use of kinetic models (2), (3) to determine the velocity of motion of the interphase boundary $v(T_{s\ell})$ not only in the area of crystallization but also melting, taking into account the strong overheating of the solid phase.

The temperature dependence of the stationary velocity of motion of an SLI in metals at the maximum permissible values of overheating/undercooling plays a crucial role in the continuum models used in studies of heterogeneous mechanisms of melting and crystallization [18, 22].

2. MODIFIED KINETIC MODEL

The transition state theory [41] assumes that crystallization and melting proceed through an indefinite transition state, which is characterized by the presence of processes with two rates: one describes the melting rate $R_{s\to\ell}$ and the other is the solidification rate $R_{\ell\to s}$. The difference between these two velocities gives the SLI velocity

$$v_{s\ell} = R_{s\to\ell} - R_{\ell\to s}. \tag{4}$$

The intermediate state (intermediate phase), through which the forward and reverse transitions occur, has a certain Gibbs energy G^*. The driving force behind these transitions is the difference in the Gibbs energies of G^* and the corresponding phase G_s and G_ℓ, standing in the Arrhenius exponent

$$R_{s\to\ell} = \chi_s \exp[-(G^* - G_s)/k_BT], \quad R_{\ell\to s} = \chi_\ell \exp[-(G^* - G_\ell)/k_BT]. \tag{5}$$

Here, k_B is the Boltzmann constant, T is temperature, χ_s and χ_ℓ are the coefficients of proportionality, which in classical theory are assumed to be equal to each other $\chi_s = \chi_\ell = \chi$. Then the velocity of the interphase boundary has the form

$$v_{s\ell} = \chi \exp\left[-\frac{G^* - G_\ell}{k_BT}\right]\left\{\exp\left[\frac{G_s - G_\ell}{k_BT}\right] - 1\right\}. \tag{6}$$

The value of the energy barrier, which appears in the exponential before the curly bracket, can be interpreted as the activation energy of the process that limits the melting/crystallization rate. In the WF phenomenological theory [28–30], this limiting process is associated with the diffusion of atoms in a liquid, delivering atoms to the crystallization front:

$$v_{s\ell} = \chi \exp\left[-\frac{Q}{k_BT}\right]\left\{\exp\left[\frac{G_s - G_\ell}{k_BT}\right] - 1\right\}. \tag{7}$$

After performing the thermodynamic transformations of the difference between the Gibbs energies of the solid and liquid phases, the final expression, the main conclusion of the theory of the transition state in relation to diffusion-limited melting/crystallization processes, is obtained:

$$v(T_{s\ell}) = \chi \exp\left[-\frac{Q}{k_BT_{sl}}\right]\left\{\exp\left[\frac{L_m(T_{s\ell} - T_m)}{T_{s\ell}T_m}\right] - 1\right\}. \tag{8}$$

Here, T_m is the equilibrium melting temperature, $T_{s\ell}$ is the temperature of the melting front, and L_m is the latent heat of fusion at temperature T_m.

Equation (8) showed an acceptable coincidence of the rates in the region of crystallization and melting in a small vicinity of the equilibrium temperature T_m with the MD simulation results and experimental data. However, in a wide temperature range, in which melting/crystallization processes can occur with the maximum permissible values of overheating/undercooling, it was not possible to obtain acceptable agreement, since the kinetics of melting/crystallization far from the temperature T_m differs significantly from the kinetics in the vicinity of T_m.

To overcome this difficulty, it became necessary to modify the WF kinetic model [28–30] with diffusion limitation (8). The proposed modification is based on the assumption of the asymmetry of the processes of direct and reverse transitions (5) in the transition state. The simplest form of asymmetry can be represented as the lack of equality of the proportionality coefficients $\chi_s \neq \chi_\ell$ and the ratio χ_s/χ_ℓ in the form

of a functional dependence on temperature $f(T_{s\ell})$. Taking into account the relation χ_s/χ_ℓ, the expression for velocity (6) can be represented as

$$v_{s\ell} = \chi_\ell \exp\left[-\frac{G^* - G_\ell}{k_B T}\right]\left\{\frac{\chi_s}{\chi_\ell}\exp\left[\frac{G_s - G_\ell}{k_B T}\right] - 1\right\}. \quad (9)$$

Or, repeating the reasoning given above,

$$v(T_{s\ell}) = \chi_\ell \exp\left[-\frac{Q}{k_B T_{s\ell}}\right]\left\{\frac{\chi_s}{\chi_\ell}\exp\left[\frac{L_m (T_{s\ell} - T_m)}{k_B T_{s\ell} T_m}\right] - 1\right\}. \quad (10)$$

When determining the functional dependence $\chi_s/\chi_\ell = f(T_{s\ell})$, we use the following considerations. The ratio χ_s/χ_ℓ in the general case is different from unity. However, in a state of equilibrium, when the equalities $T_{s\ell} = T_m$ and, correspondingly, $G_s = G_\ell$ are satisfied, the expressions in curly brackets in (9), (10) must vanish. This means that the functional dependence $\chi_s/\chi_\ell = f(T_{s\ell})$ should take a value equal to unity in a state of equilibrium. As such a dependence, satisfying the condition $\chi_s/\chi_\ell = 1$, we can use the relation

$$\frac{\chi_s}{\chi_\ell} = \exp\left[\alpha\frac{T_{s\ell} - T_m}{T_m}\right], \quad (11)$$

where α is the dimensionless coefficient to be determined.

Taking into account expression (11), the modified model with diffusion limitation takes the final form

$$v(T_{s\ell}) = \chi_\ell \exp\left[-\frac{Q}{k_B T_{s\ell}}\right]\left\{\exp\left[\left(\frac{L_m}{k_B T_{s\ell}} + \alpha\right)\frac{T_{s\ell} - T_m}{T_m}\right] - 1\right\}, \quad (12)$$

where χ_ℓ [m/sec] is a dimensional constant depending on the crystallographic orientation interface to be defined.

The modified equation (12) contains 3 constants χ_ℓ, Q, and α, whose values are determined by comparison with the results of the MD calculations followed by the application of the least squares method [42].

3. SETTING UP A COMPUTATIONAL EXPERIMENT (CE) AND MODELING

The stationary temperature dependence of the kinetic velocity of an SLI in the range of the maximum permissible values of overheating/undercooling was determined using a computational experiment consisting of a large series of MD calculations.

Two types of metals were used in the simulation: Al and Cu with an FCC lattice and Fe with a BCC lattice. Al was considered in two crystallographic planes: ⟨100⟩ and ⟨111⟩. Atomistic models are based on the model idea of a polyatomic molecular system, in which all atoms are represented by material points, whose motion is described in the classical case by Newton's equations. As a result, the evolution of the ensemble from N point particles are determined by a system of $2N$ ordinary differential equations. The interaction between particles is described by various multiparticle potentials of the embedded atom method (EAM): for aluminum [43], copper [44], and iron [45] with parameterization [46]. To integrate this system of equations for all N particles requires knowledge of the coordinates and velocities $(r_i, v_i)\big|_{t=0}$ at the initial moment of time $t = 0$. The computational domain was specified in the form of a parallelepiped with dimensions of 41 × 5 × 5 nm, which corresponds to 20 × 10 × 10 unit cells containing 57 600 particles. In all three spatial directions, the periodic boundary conditions were set at the boundaries of the computational domain; i.e., the simulated object was an infinite single crystal of metal.

The initial state of the computational domain for modeling the process of heterogeneous metal melting is a solid structure with a liquid layer in the middle of the computational domain, in which the crystalline and liquid phases are separated by two flat interfaces. To study the melting process, the liquid phase occupies approximately 18% of the volume of the computational domain; and to study the crystallization process, ~80%. Subsequently, the velocity of the interface was directly measured depending on its temperature.

In the calculations using a thermostat, a fixed temperature value was established and maintained throughout the entire computational domain throughout the numerical experiment. At the same time, the barostat maintained a constant value of external pressure. This excluded the reverse influence of the

release/absorption of latent heat of fusion on the local temperature at the fronts. As a result, the process of heterogeneous melting/crystallization quickly reaches a stationary regime, and the change in the amount of the new phase occurs almost according to a linear law. The position of the melting/crystallization fronts was tracked using the order parameter.

The maximum permissible values of overheating/undercooling mean the temperature values at which, in the event of overheating, the original crystal still retains its mechanical stability, whose loss is related to the onset of homogeneous melting. For the stationary exposure conditions, the value of the maximum overheating at $T_{s\ell} \approx 1.25T_m$, which is in close agreement with the results of [7, 14, 15]. In the nonstationary exposure, the limiting value of overheating reached a value of $1.5T_m$ or higher, which coincides with the estimates [47].

In the case of supercooling, the limiting temperature is the temperature at which the supercooled melt is still a pure liquid. The limitation of deep penetration into the metastable supercooled region is related to the formation of an intermediate (interstitial) phase, for which the order parameter turns out to be significantly larger than that of a liquid, but significantly smaller than that of a normal crystal. The appearance of the interstitial phase indicates the beginning of the glass transition process. The glass transition temperature for most metals is in the range $T_c \approx (0.3–0.5)T_m$ [34]. The calculation variants in which a noticeable proportion of the interstitial phase appeared were excluded from consideration.

4. ATOMISTIC MODELING RESULTS

As a result of the MD simulation, a discrete set of values of the phase front velocity $v_{\langle hk\ell\rangle} = v_{\langle hk\ell\rangle,i}$ was obtained at temperatures $T_{s\ell} = T_i$ ($i = 0–n$, n is the number of discrete values obtained from the MD simulation). The phase front velocities $v_{\langle hk\ell\rangle,i}$ were obtained depending on the crystallographic orientation of the interface: for Al, $v_{\langle 100\rangle,i}$, $v_{\langle 111\rangle,i}$ and for Cu and Fe, $v_{\langle 100\rangle,i}$ within the range of overheating/undercooling limit values. The pairs of discrete values $\{v_{\langle hk\ell\rangle,i}, T_i\}$ in Figs. 1 and 2 are marked with markers.

4.1. Construction of Analytical Dependencies $v_{\langle hk\ell\rangle}(T_{s\ell})$

The analytical dependences were constructed using the least squares method.

The discrete set of values $\{v_{\langle hk\ell\rangle,i}, T_i\}$ obtained from the MD simulations was compared with the results of a modified kinetic model (12). In the comparison, it was taken into account that Eq. (12) contains two thermophysical parameters, the equilibrium melting temperature T_m and latent heat of fusion L_m, whose values, due to the characteristics of the interaction potentials used in the MD calculations, may differ slightly from the reference ones. To correctly compare the MD data with the kinetic data in Eq. (12), we used the T_m and L_m values determined for all the considered metals Al, Cu, and Fe from the additional

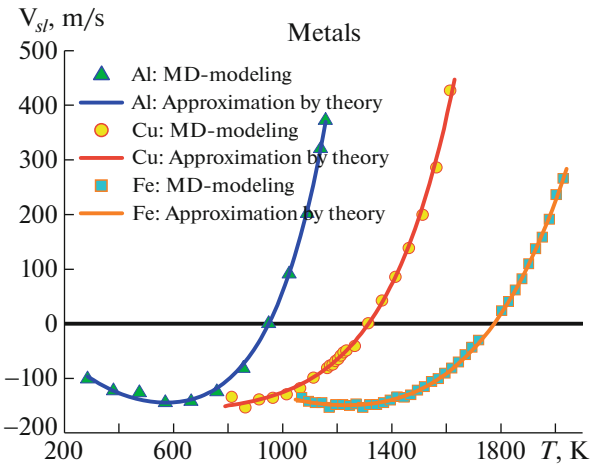

Fig. 1. Dependences of the stationary SLI rate for Al, Cu, Fe on the overheating temperature of the initial phase in the crystallographic plane ⟨100⟩.

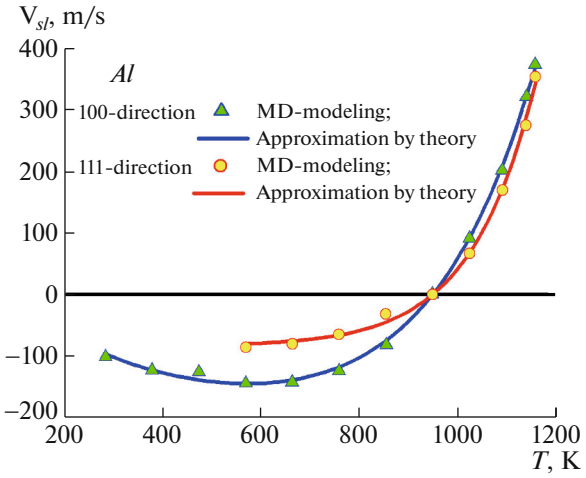

Fig. 2. Dependence of the SLI rate for Al in crystallographic planes ⟨100⟩ and ⟨111⟩ on the temperature at the phase front $T_{s\ell}$ at $P = 0$.

MD calculations performed using the method from [48] with the same potentials [43–46]. The calculation results T_m and L_m for external pressure $P = 0$ are given in Table 1.

The discrete set of values $\{v_{\langle hk\ell\rangle,i}, T_i\}$ was completely combined with the results of Eq. (12) $v_{\langle hk\ell\rangle}(T_{s\ell})$ using a three-parameter (χ_ℓ, Q, α) approximation.

The best agreement with an error not exceeding a few percent over the entire temperature range was achieved with the values of the approximating parameters χ_ℓ, Q, and α in (12), presented in Table 2. To determine them, a procedure containing the least squares criterion σ was used [42], which minimizes the deviation of the values of Eq. (12) $v_{\langle hk\ell\rangle}(T_i)$ with selected parameters from the results of the MD simulation $\{v_{\langle hk\ell\rangle,i}, T_i\}$

$$\sigma = \sqrt{(1/n+1)\sum_{i=0}^{n}\left(v_{\langle hk\ell\rangle}(T_i) - v_{\langle hk\ell\rangle,i}\right)^2} \to \min.$$

Table 2 also shows the values of the least squares criterion σ and σ^*, calculated for each of the interaction potentials in this study and in [49]. In [49], for the original WF (2) models [28–30], approximations of the phase front velocity $v_{\langle hk\ell\rangle}(T_{s\ell})$ and values of the least squares criterion σ^* for metals Al, Cu, and Fe were obtained. The modification of the WF model (12) in this study made it possible to increase the accuracy of the results obtained in accordance with the least squares criterion [42] in comparison with the results of [49], which is especially noticeable for Cu and Fe. The standard deviation σ in the presented calculations decreased by 34.41% for Cu and by 22.86% for Fe (Table 2) compared to the standard deviation values of σ^* in [49].

The proposed approach was used in [50] to modify the WF model to obtain the temperature dependence of the SLI rate in silicon (Si). It is well known that the problem of choosing the particle interaction potential is the most important problem in MD modeling. This problem is especially acute for Si. In [50], calculations were carried out for the Stillinger–Weber [51] and Kumagai, Izumi, Hara, and Sakai (KIHS) [52] potentials. The simulation showed that modification of the WF model made it possible to obtain almost complete agreement between the temperature dependence of the interface velocity and the results

Table 1. Equilibrium melting point T_m and latent heat of fusion L_m from MD calculations

Metal	T_m, K	L_m, kJ/mol
Al	949	8.9
Cu	1315	11.48
Fe	1775	15.57

Table 2. Values of parameters χ_ℓ, Q, α in a three-parameter approximation of the phase front velocity $v_{\langle hk\ell\rangle}(T_{s\ell})$ and the values of the least squares criterion σ

Metal	Modified model				Work [49]	$\lvert\sigma - \sigma^*\rvert/\sigma$, %
	χ_ℓ, m/s	Q, eg	α	σ, m/s	σ^*, m/s	
$Al_{[100]}$	269.93	0.02510	3.6930	5.513	5.82	5.57
$Al_{[111]}$	82.97	0.0	6.5076	7.105		
Cu	169.47	0.002317	4.585845	7.961	10.70	34.41
Fe	558.706	0.1154158	3.6309	3.150	3.87	22.86

of MD simulation for both potentials. The results for metals Al, Cu, and Fe obtained in this study, in combination with the previously obtained results for Si [50], allowed us to formulate a unified model for approximating the temperature dependence of the SLI rate (12) for metals and semiconductors, which is an important step to ensure continuum models with kinetic properties.

Figure 1 shows the velocity dependences SLI $v_{\langle hk\ell\rangle}(T_i)$ in the crystallographic plane $\langle 100\rangle$ of Al, Cu, and Fe and velocity dependences SLI $v_{\langle hk\ell\rangle}(T_i)$ in crystallographic planes $\langle 100\rangle$ and $\langle 111\rangle$ for Al (Fig. 2) at an external pressure of $P = 0$.

Note that when modeling the crystallization process of aluminum in the region of significant overcooling of the interface with orientation $\langle 111\rangle$ the likelihood of packaging defects significantly increases. Their accumulation leads to distortion of the original crystallographic plane, and the further propagation of the front occurs in a direction different from $\langle 111\rangle$. For this reason, in the crystallographic direction $\langle 111\rangle$, the overcooling region below $0.6T_m$ could not be reached.

5. BRIEF ANALYSIS OF THE RESULTS OBTAINED

The resulting $v_{\langle 100\rangle}(T_{s\ell})$ curves, characterizing the SLI mobility for the considered FCC and BCC metals in the crystallographic plane $\langle 100\rangle$, have a great deal in common. The melting branches in the range $T_m \le T_{s\ell} \le 1.25T_m$ have exponential behavior as overheating increases, reaching maximum values of $v_{\langle 100\rangle}(T_{s\ell}) \sim 300-350$ m/sec. The crystallization process in the supercooling region $0.5T_m \le T_{s\ell} \le T_m$ is more complicated. The crystallization rate $v(T_{s\ell})$ on all curves in Figs. 1 and 2 in the area of $T_{s\ell} \sim 0.7T_m$ has a clearly visible maximum of ~140–160 m/sec. It should be noted that the maximum rate of Fe crystallization coincides with the analogous data obtained in [41]. The appearance of the maximum crystallization rate is related to the beginning of the formation of an interstitial phase, which slows down the velocity of the phase front. Ours considers only crystallization processes in insufficiently cooled pure liquid. Glass transition processes occurring near and below temperature T_g, $0 < T_{s\ell} \le T_g$ are not included because the complexity and importance of this process, particularly for technological applications, deserve separate consideration.

It should be noted that the mobility of SLI is greatly influenced by its crystallographic orientation. For example, for aluminum the ratio of the maximum crystallization rates reaches $v_{\langle 100\rangle}(T_{s\ell})/v_{\langle 111\rangle}(T_{s\ell}) \approx 2$; and of the melting rate, 1.2 (Fig. 2).

6. CONCLUSIONS

The kinetics of melting/crystallization of FCC and BCC of metals Al, Cu, and Fe in the range of extreme values of overheating/undercooling was studied using the molecular dynamics method. The maximum overheating/undercooling for each metal is determined by the temperature values at which the overheated crystal retains the properties of the crystal, and the overcooled melt remains liquid.

(a) A radical modification of the WF kinetic model was performed [28–30], reflecting the asymmetry of the melting and solidification processes. The use of the modified model (12) made it possible for metals Al, Cu, and Fe to obtain analytical expressions for the velocity of propagation of the SLI in the range of extreme overheating/undercooling with significantly higher accuracy compared to the results obtained in [49] for the original WF models [28–30].

(b) The discrete set of velocity values $\{v_{\langle hk\ell\rangle,i}, T_i\}$ obtained as a result of atomistic modeling was used to construct analytical dependencies of the stationary velocity of motion of the SLI of $v_{\langle hk\ell\rangle}(T_{s\ell})$ (12) over the entire range of overheating/undercooling limit values.

(c) The simulation results showed that for the metals under consideration the range of overheating/undercooling limit values is as follows:

for $Al_{\langle 100\rangle}$, $T_{s\ell} \approx (0.3–1.25)T_m$, for $Al_{\langle 111\rangle}$, $T_{s\ell} \approx (0.6–1.2)T_m$,

for Cu, $T_{s\ell} \approx (0.6–1.3)T_m$, and for Fe, $T_{s\ell} \approx (0.5–1.18)T_m$.

(d) The temperature dependencies of the SLI velocity for Al, Cu, and Fe, determined from simulation results using different crystallographic planes, demonstrate a clear asymmetry with respect to the melting point T_m, which is explained by the strong difference between the kinetics of melting in a highly overheated state and the kinetics of solidification in a highly supercooled state.

(e) The obtained temperature dependence of the velocity of motion of the interphase boundary is diffusion-limited and is described by the same equation for each metal over the entire temperature range. For all metals, the change in the temperature dependence of the velocity $v(T_{s\ell})$ when passing through the melting point T_m occurs smoothly, without a bend in the slope.

(f) The crystallographic orientation of the metal, and not the type of its crystal lattice, has the greatest influence on the mobility of the interphase boundary.

FUNDING

This study was supported by the Russian Science Foundation, project no. 18-11-00318.

The results were obtained using the equipment of Shared Resource Center of the Keldysh Institute of Applied Mathematics of the Russian Academy of Sciences.

CONFLICT OF INTEREST

The authors of this work declare that they have no conflicts of interest.

REFERENCES

1. *Handbook of Materials Modeling*, Ed. by S. Yip (Springer, Dordrecht, 2005). https://doi.org/10.1007/978-1-4020-3286-8
2. A. L. Pirozerski, O. I. Smirnova, A. I. Nedbai, O. L. Pirozerskaya, N. A. Grunina, and V. M. Mikushev, "Peculiarities of melting and crystallization of n-decane in a porous glass," Phys. Lett. A **383**, 125872 (2019). https://doi.org/10.1016/j.physleta.2019.125872
3. J. F. Van der Veen, "Melting and freezing at surfaces," Surf. Sci. **433–435**, 1–11 (1999). https://doi.org/10.1016/s0039-6028(99)00084-9
4. B. J. Siwick, J. R. Dwyer, R. E. Jordan, and R. J. D. Miller, "An atomic-level view of melting using femtosecond electron diffraction," Science **302**, 1382–1385 (2003). https://doi.org/10.1126/science.1090052
5. V. I. Mazhukin, "Kinetics and dynamics of phase transformations in metals under action of ultra-short high-power laser pulses," in *Laser Pulses–Theory, Technology, and Applications*, Ed. by I. Peshko (InTech, Rijeka, Croatia, 2012), pp. 219–276. https://doi.org/10.5772/50731
6. M. Li, Sh. Ozawa, and K. Kuribayashi, "On determining the phase-selection principle in solidification from undercooled melts—Competitive nucleation or competitive growth?," Philos. Mag. Lett. **84**, 483–493 (2004). https://doi.org/10.1080/0950083042000271090
7. Q. S. Mei and K. Lu, "Melting and superheating of crystalline solids: From bulk to nanocrystals," Prog. Mater. Sci. **52**, 1175–1262 (2007). https://doi.org/10.1016/j.pmatsci.2007.01.001
8. A. B. Belonoshko, N. V. Skorodumova, A. Rosengren, and B. Johansson, "Melting and critical superheating," Phys. Rev. B **73**, 012201 (2006). https://doi.org/10.1103/physrevb.73.012201
9. N. A. Berjeza, S. P. Velikevitch, V. I. Mazhukin, I. Smurov, and G. Flamant, "Influence of temperature gradient to solidification velocity ratio on the structure transformation in pulsed- and CW-laser surface treatment," Appl. Surf. Sci. **86**, 303–309 (1995). https://doi.org/10.1016/0169-4332(94)00446-3

10. M. Asta, C. Beckermann, A. Karma, W. Kurz, R. Napolitano, M. Plapp, G. Purdy, M. Rappaz, and R. Trivedi, "Solidification microstructures and solid-state parallels: Recent developments, future directions," Acta Mater. **57**, 941–971 (2009).
https://doi.org/10.1016/j.actamat.2008.10.020

11. P. K. Galenko and D. V. Alexandrov, "From atomistic interfaces to dendritic patterns," Philos. Trans. R. Soc. A: Math., Phys. Eng. Sci. **376**, 20170210 (2018).
https://doi.org/10.1098/rsta.2017.0210

12. M. V. Shugaev, M. He, S. A. Lizunov, Yo. Levy, Th. J.-Y. Derrien, V. P. Zhukov, N. M. Bulgakova, and L. V. Zhigilei, "Insights into laser-materials interaction through modeling on atomic and macroscopic scales," in *Advances in the Application of Lasers in Materials Science*, Ed. by P. M. Ossi, Springer Series in Materials Science, Vol. 274 (Springer, Cham, 2018), pp. 107–148.
https://doi.org/10.1007/978-3-319-96845-2_5

13. D. V. Sivukhin, *General Course of Physics in Five Volumes*, Vol. 2: *Thermodynamics and Molecular Physics* (Fizmatlit, Moscow, 2005).

14. V. I. Mazhukin, O. N. Koroleva, A. V. Shapranov, A. A. Aleksashkina, and M. M. Demin, "Molecular dynamics study of thermal hysteresis during melting-crystallization of noble metals," Math. Montisnigri **53**, 89–99 (2022).
https://doi.org/10.20948/mathmontis-2022-53-8

15. V. I. Mazhukin, O. N. Koroleva, A. V. Shapranov, M. M. Demin, and A. A. Aleksashkina, "Determination of thermal properties of gold in the region of melting–crystallization phase transition: Molecular dynamics approach," Math. Models Comput. Simul. **14**, 662–676 (2022).
https://doi.org/10.1134/s2070048222040068

16. J. Cheng, C. Liu, S. Shang, D. Liu, W. Perrie, G. Dearden, and K. Watkins, "A review of ultrafast laser materials micromachining," Opt. Laser Technol. **46**, 88–102 (2013).
https://doi.org/10.1016/j.optlastec.2012.06.037

17. J. Yan, P. Liu, Z. Lin, H. Wang, H. Chen, C. Wang, and G. Yang, "Directional Fano resonance in a silicon nanosphere dimer," ACS Nano **9**, 2968–2980 (2015).
https://doi.org/10.1021/nn507148z

18. V. I. Mazhukin, M. M. Demin, and A. V. Shapranov, "High-speed laser ablation of metal with pico- and subpicosecond pulses," Appl. Surf. Sci. **302**, 6–10 (2014).
https://doi.org/10.1016/j.apsusc.2014.01.111

19. M. Cesaria, A. P. Caricato, M. Beccaria, A. Perrone, M. Martino, A. Taurino, M. Catalano, V. Resta, A. Klini, and F. Gontad, "Physical insight in the fluence-dependent distributions of Au nanoparticles produced by subpicosecond UV pulsed laser ablation of a solid target in vacuum environment," Appl. Surf. Sci. **480**, 330–340 (2019).
https://doi.org/10.1016/j.apsusc.2019.02.022

20. A. Menéndez-Manjón, S. Barcikowski, G. A. Shafeev, V. I. Mazhukin, and B. N. Chichkov, "Influence of beam intensity profile on the aerodynamic particle size distributions generated by femtosecond laser ablation," Laser Part. Beams **28**, 45–52 (2010).
https://doi.org/10.1017/s0263034609990553

21. J. H. Perepezko and G. Wilde, "Melt undercooling and nucleation kinetics," Curr. Opin. Solid State Mater. Sci. **20**, 3–12 (2016).
https://doi.org/10.1016/j.cossms.2015.07.001

22. V. I. Mazhukin, A. V. Shapranov, V. E. Perezhigin, O. N. Koroleva, and A. V. Mazhukin, "Kinetic melting and crystallization stages of strongly superheated and supercooled metals," Math. Models Comput. Simul. **9**, 448–456 (2016).
https://doi.org/10.1134/s2070048217040081

23. Yu. Ch. Shen and D. W. Oxtoby, "Density functional theory of crystal growth: Lennard-Jones fluids," J. Chem. Phys. **104**, 4233–4242 (1996).
https://doi.org/10.1063/1.471234

24. M. I. Mendelev, M. J. Rahman, J. J. Hoyt, and M. Asta, "Molecular-dynamics study of solid–liquid interface migration in fcc metals," Modell. Simul. Mater. Sci. Eng. **18**, 074002 (2010).
https://doi.org/10.1088/0965-0393/18/7/074002

25. V. I. Mazhukin, A. V. Shapranov, M. M. Demin, and N. A. Kozlovskaya, "Temperature dependence of the kinetics rate of the melting and crystallization of aluminum," Bull. Lebedev Phys. Inst. **43**, 283–286 (2016).
https://doi.org/10.3103/s1068335616090050

26. V. I. Mazhukin, A. V. Shapranov, V. E. Perezhigin, O. N. Koroleva, and A. V. Mazhukin, "Kinetic melting and crystallization stages of strongly superheated and supercooled metals," Math. Models Comput. Simul. **9**, 448–456 (2017).
https://doi.org/10.1134/s2070048217040081

27. C. J. Tymczak and J. R. Ray, "Asymmetric crystallization and melting kinetics in sodium: A molecular-dynamics study," Phys. Rev. Lett. **64**, 1278–1281 (1990).
https://doi.org/10.1103/physrevlett.64.1278

28. H. A. Wilson, "XX. On the velocity of solidification and viscosity of super-cooled liquids," London, Edinburgh, Dublin Philos. Mag. J. Sci. **50**, 238–250 (1900).
https://doi.org/10.1080/14786440009463908

29. Ja. I. Frenkel, "Note on the relation between the speed of crystallization and viscosity," Phys. Z. Sowjet Union **1**, 498–499 (1932).

30. J. Frenkel, *Kinetic Theory of Solids* (Oxford Univ. Press, New York, 1946).

31. J. Q. Broughton, G. H. Gilmer, and K. A. Jackson, "Crystallization rates of a Lennard-Jones liquid," Phys. Rev. Lett. **49**, 1496–1500 (1982).
https://doi.org/10.1103/physrevlett.49.1496

32. K. A. Jackson, "The interface kinetics of crystal growth processes," Interface Sci. **10**, 159–169 (2002).
https://doi.org/10.1023/a:1015824230008

33. L. V. Mikheev and A. A. Chernov, "Mobility of a diffuse simple crystal—melt interface," J. Cryst. Growth **112**, 591–596 (1991).
https://doi.org/10.1016/0022-0248(91)90340-b

34. Y. Ashkenazy and R. S. Averback, "Kinetic stages in the crystallization of deeply undercooled body-centered-cubic and face-centered-cubic metals," Acta Mater. **58**, 524–530 (2010).
https://doi.org/10.1016/j.actamat.2009.09.030

35. D. Turnbull, "On the relation between crystallization rate and liquid structure," J. Phys. Chem. **66**, 609–613 (1962).
https://doi.org/10.1021/j100810a009

36. Y. Ashkenazy and R. S. Averback, "Atomic mechanisms controlling crystallization behaviour in metals at deep undercoolings," Europhys. Lett. **79**, 26005 (2007).
https://doi.org/10.1209/0295-5075/79/26005

37. C. A. Macdonald, A. M. Malvezzi, and F. Spaepen, "Picosecond time-resolved measurements of crystallization in noble metals," J. Appl. Phys. **65**, 129–136 (1989).
https://doi.org/10.1063/1.342586

38. W. L. Chan, R. S. Averback, D. G. Cahill, and Y. Ashkenazy, "Solidification velocities in deeply undercooled silver," Phys. Rev. Lett. **102**, 095701 (2009).
https://doi.org/10.1103/PhysRevLett.102.095701

39. M. I. Mendelev, "Molecular dynamics simulation of solidification and devitrification in a one-component system," Modell. Simul. Mater. Sci. Eng. **20**, 045014 (2012).
https://doi.org/10.1088/0965-0393/20/4/045014

40. M. D. Kluge and J. R. Ray, "Velocity versus temperature relation for solidification and melting of silicon: A molecular-dynamics study," Phys. Rev. B **39**, 1738–1746 (1989).
https://doi.org/10.1103/physrevb.39.1738

41. K. A. Jackson and B. Chalmers, "Kinetics of solidification," Can. J. Phys. **34**, 473–490 (1956).
https://doi.org/10.1139/p56-054

42. A. A. Samarskii and A. V. Gulin, *Numerical Methods* (Fizmatlit, Moscow, 1989).

43. V. V. Zhakhovskii, N. A. Inogamov, Yu. V. Petrov, S. I. Ashitkov, and K. Nishihara, "Molecular dynamics simulation of femtosecond ablation and spallation with different interatomic potentials," Appl. Surf. Sci. **255**, 9592–9596 (2009).
https://doi.org/10.1016/j.apsusc.2009.04.082

44. S. M. Foiles, M. I. Baskes, and M. S. Daw, "Embedded-atom-method functions for the fcc metals Cu, Ag, Au, Ni, Pd, Pt, and their alloys," Phys. Rev. B **33**, 7983–7991 (1986).
https://doi.org/10.1103/physrevb.33.7983

45. M. I. Mendelev, S. Han, D. J. Srolovitz, G. J. Ackland, D. Y. Sun, and M. Asta, "Development of new interatomic potentials appropriate for crystalline and liquid iron," Philos. Mag. **83**, 3977–3994 (2003).
https://doi.org/10.1080/14786430310001613264

46. G. J. Ackland, M. I. Mendelev, D. J. Srolovitz, S. Han, and A. V. Barashev, "Development of an interatomic potential for phosphorus impurities in α-iron," J. Phys.: Condens. Matter **16**, S2629–S2642 (2004).
https://doi.org/10.1088/0953-8984/16/27/003

47. B. Rethfeld, K. Sokolowski-Tinten, D. von der Linde, and S. I. Anisimov, "Ultrafast thermal melting of laser-excited solids by homogeneous nucleation," Phys. Rev. B **65**, 092103 (2002).
https://doi.org/10.1103/physrevb.65.092103

48. V. I. Mazhukin, A. V. Shapranov, and V. E. Perezhigin, "Mathematical modeling of thermophysical properties, metal heating and melting processes by molecular dynamics method," Math. Montisnigri **24**, 47–66 (2012).
49. V. I. Mazhukin, A. V. Shapranov, and O. N. Koroleva, "Atomistic modeling of crystal-melt interface mobility of fcc (Al, Cu) and bcc (Fe) metals in strong superheating/undercooling states," Math. Montisnigri **48**, 70–85 (2020).
https://doi.org/10.20948/mathmontis-2020-48-7
50. V. I. Mazhukin, A. V. Shapranov, A. V. Mazhukin, and P. V. Breslavsky, "Atomistic modeling of the dynamics of the solid–liquid interface for the melting and crystallization of Si under deeply superheated/supercooled states," Math. Montisnigri **47**, 87–99 (2020).
https://doi.org/10.20948/mathmontis-2020-47-8
51. F. H. Stillinger and T. A. Weber, "Computer simulation of local order in condensed phases of silicon," Phys. Rev. B **31**, 5262–5271 (1985).
https://doi.org/10.1103/physrevb.31.5262
52. T. Kumagai, S. Izumi, S. Hara, and S. Sakai, "Development of bond-order potentials that can reproduce the elastic constants and melting point of silicon for classical molecular dynamics simulation," Comput. Mater. Sci. **39**, 457–464 (2007).
https://doi.org/10.1016/j.commatsci.2006.07.013